iScience

CellPress
OPEN ACCESS

Article

Wisdom of the crowds: A suggested polygenic plan for small-RNA-mediated regulation in bacteria

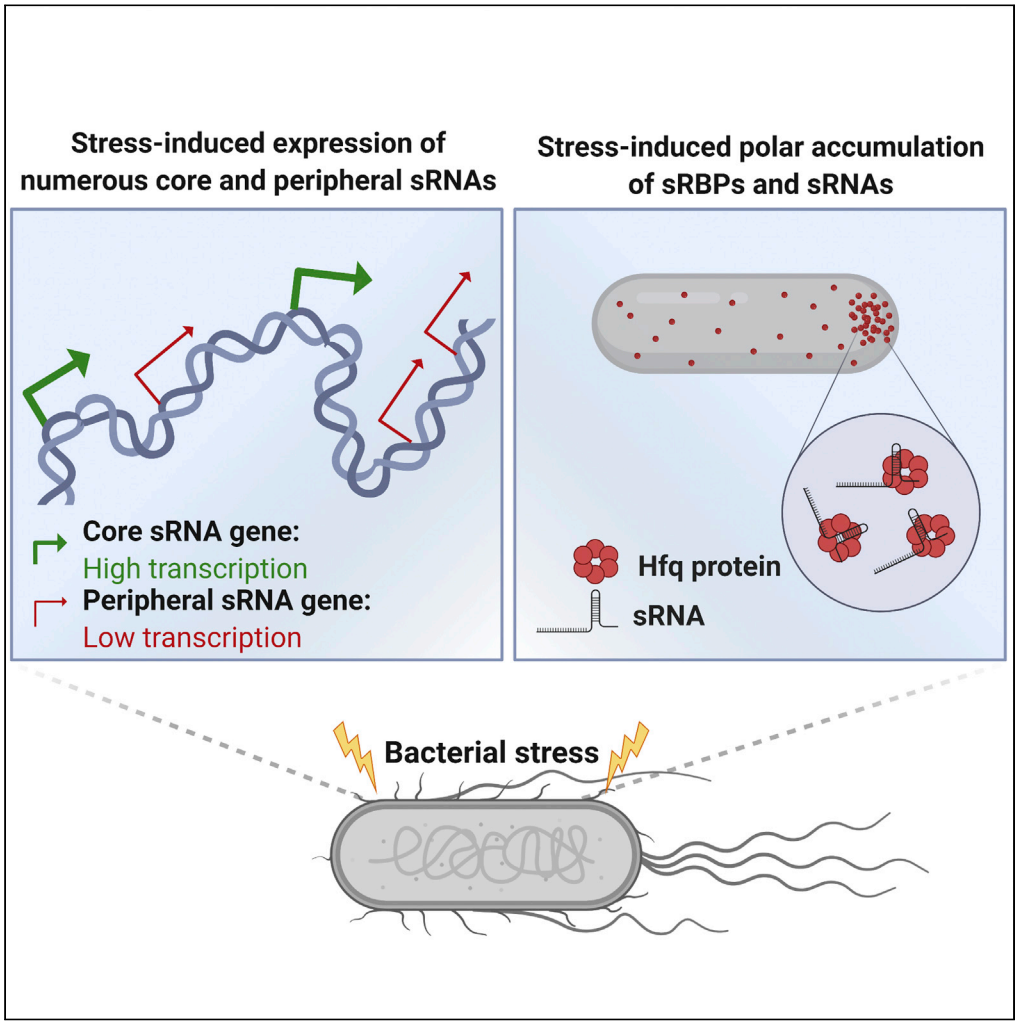

Omer Goldberger, Jonathan Livny, Roby Bhattacharyya, Orna Amster-Choder

ornaam@ekmd.huji.ac.il

Highlights

The level of numerous sRNAs increases upon various environmental conditions

Cells deleted for five pole-enriched sRNAs show a fitness defect in various stresses

No fitness defect is detected with single, double, or triple sRNA knockouts

Our data support the existence of a polygenic plan for sRNA-mediated regulation

Goldberger et al., iScience 24, 103096
October 22, 2021
https://doi.org/10.1016/j.isci.2021.103096

iScience

CellPress
OPEN ACCESS

Article

Wisdom of the crowds: A suggested polygenic plan for small-RNA-mediated regulation in bacteria

Omer Goldberger,[1] Jonathan Livny,[2] Roby Bhattacharyya,[2] and Orna Amster-Choder[1,3,*]

SUMMARY

The omnigenic/polygenic theory, which states that complex traits are not shaped by single/few genes, but by situation-specific large networks, offers an explanation for a major enigma in microbiology: deletion of specific small RNAs (sRNAs) playing key roles in various aspects of bacterial physiology, including virulence and antibiotic resistance, results in surprisingly subtle phenotypes. A recent study uncovered polar accumulation of most sRNAs upon osmotic stress, the majority not known to be involved in the applied stress. Here we show that cells deleted for a handful of pole-enriched sRNAs exhibit fitness defect in several stress conditions, as opposed to single, double, or triple sRNA-knockouts, implying that regulation by sRNA relies on sets of genes. Moreover, analysis of RNA-seq data of *Escherichia coli* and *Salmonella typhimurium* exposed to antibiotics and/or infection-relevant conditions reveals the involvement of multiple sRNAs in all cases, in line with the existence of a polygenic plan for sRNA-mediated regulation.

INTRODUCTION

Bacteria occupy different niches on our planet and in our body, where they need to adapt to and survive in rapidly fluctuating conditions. One mechanism that assists bacteria to cope with acute environmental changes (hereafter termed stress) involves regulatory small RNAs (sRNA), which are present in a wide array of bacterial species. sRNAs contribute mainly to posttranscriptional control (RNA degradation or translation) by pairing with target mRNAs, with which they share varying degrees of complementarity (Storz et al., 2011). sRNAs have been extensively studied with regard to their abundance and prevalence, as well as their effect on gene expression (Hör et al., 2020) and linkage to virulence (Papenfort and Vogel, 2010; Quereda and Cossart, 2017). Their participation in transcriptional regulatory networks that control myriad microbial processes in normal growth and under stress conditions has been well documented (Holmqvist and Wagner, 2017) and continues to be revealed by high-throughput sequencing studies (Holmqvist et al., 2016, 2018; Melamed et al., 2016, 2020). The capability of several sRNAs to impact bacterial lifestyle upon their overexpression, e.g., biofilm formation and swarming (Bak et al., 2015), contributed to the notion that sRNA-mediated regulation is of major importance.

Despite the widespread roles assigned to them, only in rare cases have sRNAs been found to be essential for bacterial survival (Chen et al., 2012) and virulence (Storz et al., 2011) (Westermann, 2018). More than 300 virulence-related sRNA knockout and knockdown mutants have been examined for virulence defects in cell culture and/or in model organisms, and the vast majority (89%) exhibited no phenotype (Westermann, 2018). Some of these results might be due to the mutant strains not having been grown under the specific conditions during which the deleted or inhibited sRNAs are required. Still, the subtle effect of sRNA interference raises the question of whether and when sRNA-mediated regulation is of high importance to bacterial survival. Is the role of sRNAs limited to fine-tuning of bacterial adaptations? Is the level of redundancy among sRNAs so high that the function of all sRNAs can be fully carried out by others? Or, do sRNAs exert their effect in concert, coordinating their activity in such a way that their collective functions become essential for survival even though they are dispensable individually?

The aforementioned questions resonate on a general enigma in genetics: How come deletion or suppression of most genes, some considered essential, in different model organisms, result in no or mild phenotypes (Winzeler et al., 1999)? Already at the beginning of the 20th century, one of the founders of population genetics, R. A. Fisher, proposed that complex traits are not determined by single genes, but rather by

[1]Department of Microbiology and Molecular Genetics, IMRIC, The Hebrew University Faculty of Medicine, P.O.Box 12272, Jerusalem 91120, Israel

[2]Infectious Disease and Microbiome Program, Broad Institute of MIT and Harvard, 415 Main Street, Cambridge, MA 02140, USA

[3]Lead contact

*Correspondence: ornaam@ekmd.huji.ac.il

https://doi.org/10.1016/j.isci.2021.103096

an unlimited number of genes, each having an infinite small effect (Fisher, 2019). Such a scenario provides an explanation for the puzzling effect of single gene disruption. However, evidence for this theory could not be obtained before the revolution of next-generation sequencing (NGS), which expanded dramatically the numbers of sequenced genomes and greatly enabled their comparison. The genome-wide association studies (GWAS) performed thus far strongly suggest that multiple loci in the genome contribute to many traits (Xue et al., 2018) (Jansen et al., 2019) (Grove et al., 2019) (Ramani et al., 2012). These studies led to the emergence of the 'polygenic hypothesis,' which posits that an indefinite number of genes are involved in every trait, each having a small contribution (Barton et al., 2017). Notably, the contribution of many genes, which in most cases is marginal, becomes important under stress (Hillenmeyer et al., 2008). In 2017, Pritchard et al. proposed an expanded view, termed the 'omnigenic model,' which suggests that complex traits and diseases are influenced by interactions among all expressed genes (Boyle et al., 2017). The omnigenic/polygenic view asserts that the genes in a cell form a network with highly connected core genes, with a direct role in the process/disease, and peripheral genes, which transregulate the core genes and tip the balance.

Because the principles of regulation of gene expression are universal, and because bacteria allow little variation in chromosome length (Bergthorsson and Ochman, 1998) and, hence, in the number of genes, the polygenic plan seems most appropriate for enabling these organisms to make the most of their limited genomes. Moreover, bacteria have served as model organisms for studying gene expression for many decades (Jacob and Monod, 1961), making them ideal models for testing the polygenic theory.

The coordinated activity of many genes/transcripts, as posited by the polygenic view, can be facilitated by bringing them together in space to enable formation of regulatory networks. Transcripts colocalization-mediated posttranscriptional regulation can be certainly envisaged in eukaryotes, where the role of RNA localization in the spatiotemporal control of protein production and complex formation has been established (Basyuk et al., 2020; Chin and Lécuyer, 2017). Owing to the lack of a nucleus, posttranscriptional localization of RNA molecules has been assumed not to occur in bacterial cells and, hence, spatial organization of transcripts that may enable their synchronized activity has not been considered. However, less than a decade ago, a study from our laboratory demonstrated that bacterial mRNAs may relocate to subcellular domains where their future protein products are localized in a translation-independent manner (Nevo-Dinur et al., 2011). In a recent paper from our laboratory, it has been shown that nearly half of the *E. coli* transcriptome displays function-related extensive asymmetric distribution between the membrane, the cytoplasm, and the poles (Kannaiah et al., 2019), increasing the likelihood of spatially orchestrated activity of various transcripts in bacteria as well.

A surprising finding in the latter study was the emergence of the poles as the most unique compartment in terms of RNA composition, and the exclusive enrichment of the polar transcriptome with sRNAs (Kannaiah et al., 2019), reinforcing the idea that the poles are microbranes, as they are hubs for sensing and regulation (Amster-choder, 2011). In line with that, mRNA targets of pole-enriched sRNAs were underrepresented or overrepresented in this compartment in close compliance with the type of regulation exerted by their cognate sRNA. Notably, application of osmotic stress led to a dramatic increase in the enrichment of almost all sRNAs at the poles, i.e., two-thirds of the sRNAs were enriched by a fold change >10, with many of them showing fold change >100 and up to 650-fold (Kannaiah et al., 2019). Curiously, many of these sRNAs are not known to respond to the specific stress applied.

The surprising increase in the level of almost all sRNAs supports the existence of a polygenic plan for sRNA-mediated adaptation to stresses, with the cell poles providing a spatial arena for its implementation, which may explain the subtle effects of deleting single-sRNA genes. This hypothesis inspired us to try obtain a proof of concept for the existence of such a plan and initial identification of its features. We show here that stress application results in elevation of both stress-related and unrelated sRNAs, that exposure of bacteria to antibiotics or to infection-relevant conditions leads to changes in the level of massive numbers of sRNAs, and that we can intervene in this program and impair the bacterial ability to cope with various stresses by deleting more than a few of the sRNAs that are highly enriched at the poles upon osmotic stress, as opposed to the lack of effect after deleting individual sRNAs, twosome, or threesome. Together, our results demonstrate that large sets of sRNA genes act together under different environmental conditions and suggest that there is a spatial plan for the sRNA-mediated regulation. The demonstration that sRNAs exert their effect in concert is expected to have implications on the consideration of sRNAs, whose

involvement in major mechanisms promoting bacterial pathogenesis (Gripenland et al., 2010) and adaptation to antibiotics (Felden and Cattoira, 2018) have been documented, as players in the effort to overcome the antibiotic-resistance crisis.

RESULTS

Stress conditions induce changes in the level of numerous sRNAs

In light of the recent study, which showed that the cellular level of most sRNAs increases upon high osmolarity with no obvious correlation between the identity of the sRNAs and the stress applied (Kannaiah et al., 2019), we decided to compare the expression profile, that is, expression over time, of osmotic-stress-related and unrelated sRNAs upon the application of high osmolarity. To this end, we compared the level of sRNAs belonging to one of the following two groups at different time points after stress induction by real-time quantitative polymerase chain reaction (RT-qPCR): Group I was of sRNAs considered to be related to osmotic stress response owing to their involvement in regulating the outer membrane proteins composition – MicA, MicC, RybB, OmrA, and OmrB ((Guillier and Gottesman, 2006; Vogel and Papenfort, 2006), Figure 1A); Group II was of sRNAs not known to be related to osmotic stress – OxyS, MgrR, RyjB, SgrS, GadY, and ArcZ (Figure 1B). In our previous study, all sRNAs of Group I were significantly induced two hours after osmotic stress application (Kannaiah et al., 2019). As for Group II, the first three sRNAs – OxyS and MgrR, associated with conditions other than osmotic stress (Altuvia et al., 1997) (Moon and Gottesman, 2009) and RyjB, not associated yet with a certain condition – were at the top of the list of sRNAs whose level increased two hours after osmotic stress (Kannaiah et al., 2019). The level of the other three sRNAs in Group II increased more moderately after osmotic stress, yet their well-established connection to coping with conditions other than osmotic stress – SgrS with sugar toxicity (Vanderpool and Gottesman, 2004), GadY with low pH (Hayes et al., 2006) and ArcZ with stationary phase (Mandin and Gottesman, 2010) – were the reason for including them in this group.

The results in Figures 1A and 1B show that the level of all examined sRNAs, regardless of their linkage to osmotic stress, changed in response to high osmolarity, with each sRNA exhibiting a unique temporal pattern. Indeed, there is a difference in the average magnitude of upregulation, with two sRNAs in Group I having a maximum fold change of 3 and two others of 10, while three of the sRNAs in Group II have their maximum fold change around 2 and only one reached 10. Still, if classified based on the time their level peaked or their pattern over time, in each group there are some sRNAs that peak after a short time, 15 or 30 min, some that peak after 2 h, and some that elevate mildly and stay constant. As a control, the effect of growth *per se* on the level of the sRNAs was monitored in untreated cells (mock experiment, Figure S1). Not surprisingly, the osmotically shocked cells grew much slower than the untreated cells, reaching $0.D_{600} < 0.6$ after two hours (Figures 1A and 1B). Still, the level of the sRNAs in the faster-growing untreated cells did not increase even when the cells reached $0.D_{600} > 0.9$, that is, upon entry to stationary phase, during which expression of many sRNAs is induced (Figure S1). These results show that the changes in sRNAs level after stress application in both groups are actually related to the stress condition. Taken together, regardless of their linkage to the applied stress, expression of sRNAs from both groups was induced during osmotic stress.

Considering these and our published results, and bearing in mind the polygenic plan theory, we hypothesized that many sRNAs might be involved in multiple stresses. We, therefore, conducted a comparative analysis of RNA-seq-generated sRNA profiles before and during various stress conditions. First, we compared three data sets, obtained for the *E. coli* K12 wild-type strain MG1655 exposed to the following stress conditions: nutrient deprivation (stationary phase), iron limitation (adapted from the study by Melamed et al., 2016), and high osmolarity (RNA-seq data adapted from the study by Kannaiah et al., 2019). The three sRNA data sets are shown in Table S1. The heatmap in Figure 1C shows the level of fifty-five sRNAs monitored during the different experiments. Importantly, 12 sRNAs were significantly upregulated in response to all stress conditions, implying the existence of a broad regulatory plan for these stresses that involves common sRNAs. This finding is in line with the concept of a limited number of core genes and many peripheral genes, which underlies the polygenic plan. Hence, among the 26 sRNAs that are upregulated under iron limitation, only RyhB, previously shown to be involved in bacterial adaptation to this stress (Masse et al., 2005), was exclusively expressed in this stress, whereas 23 sRNAs were upregulated also in response to nutrient deprivation and 14 in response to high osmolarity (these numbers include the 12 that are common to the three stresses) (Figure S2). Summarily, *E. coli* response to stresses involves, and might rely on, a collection of shared and unique sRNAs.

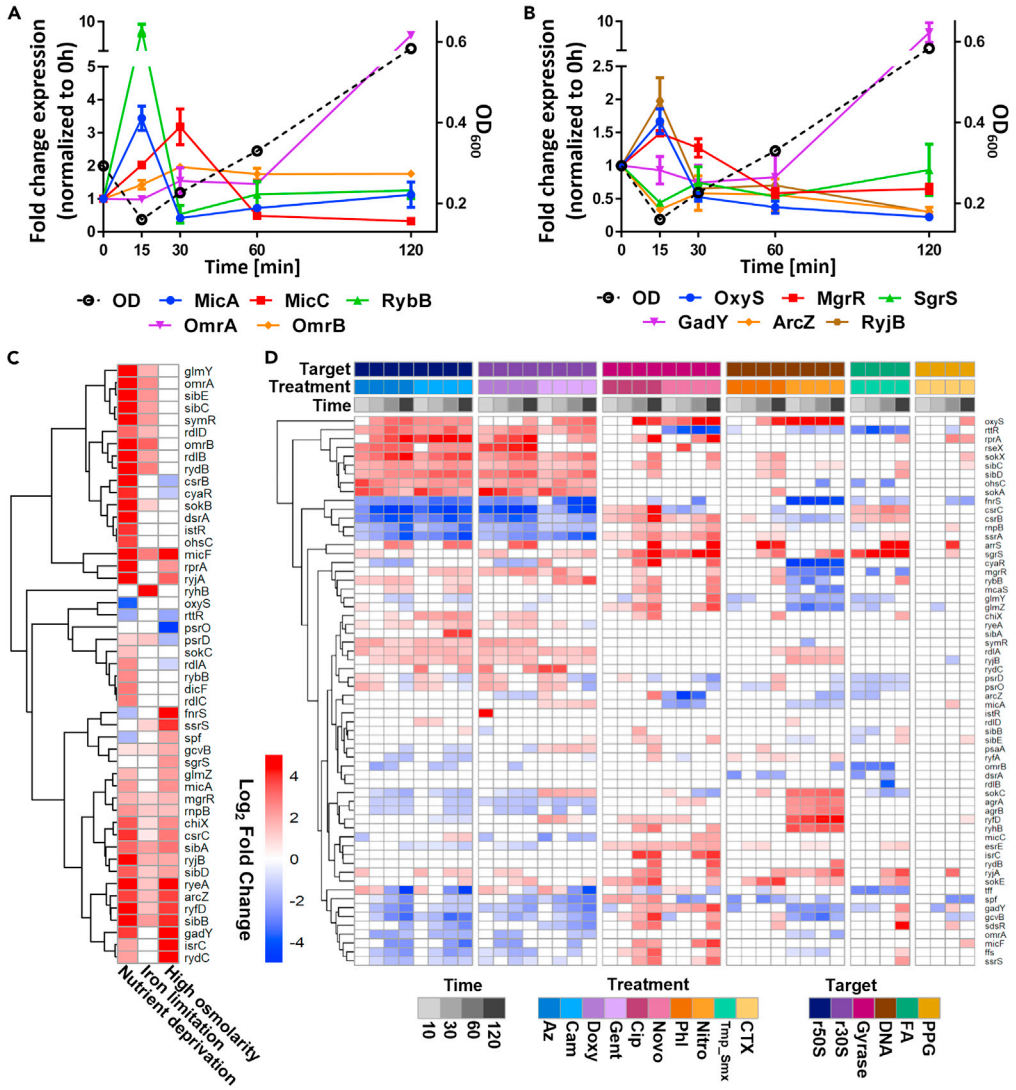

Figure 1. The level of numerous sRNAs changes in response to various stress conditions and antibiotic treatments

(A and B) Monitoring temporal expression of osmotic-stress-related (A) and nonrelated (B) sRNAs during osmotic stress (20% sucrose) of MG1655 *E. coli* cells. Expression levels in stressed vs. nonstressed were determined by qPCR, and the fold changes are given. The bars show the SEM between three biological repeats.

(C) *E. coli* sRNAs induced under stress conditions. Increase in *E. coli* sRNA levels upon high osmolarity, iron limitation, and nutrient deprivation (stationary phase) compared with the levels in non-stressed cells. See Venn diagram in Figure S2. See also *S. typhimurium* sRNAs induced under stress conditions in Figure S3.

(D) *E. coli* sRNAs induced upon antibiotic treatments. sRNA expression levels in RB001 *E. coli* cells (isolated from a patient with urinary tract infection) treated with 10 different antibiotics (4x MIC; see Table S4 for MIC values), which represent 6 groups based on their targets (indicated at the bottom) for 10, 30, 60, and 120 min compared with the sRNA levels at time 0. RNA-seq results were analyzed using DESeq2. The heatmap shows the Log_2 fold changes. Az: azithromycin, Cam: chloramphenicol, Doxy: doxycycline, Gent: gentamicin, Cip: ciprofloxacin, Novo: novobiocin, Phl: phleomycin, Nitro: nitrofurantoin, Tmp-Smx: sulfamethoxazole-trimethoprim, CTX: ceftriaxone.

The rising prevalence of bacterial resistance to antibiotics prompted us to choose them as the next example for a stress. Hence, we analyzed the changes in sRNAs expression in a clinical *E. coli* isolate after treatment with 10 different antibiotics, which represent 6 groups based on their targets at different time points up to two hours compared with their level before treatment (Table S2, see STAR Methods for generation and analysis of RNA-Seq data). Figure 1D shows patterns of increase and decrease in the level of certain sRNAs that are common to each group of antibiotics, the most noticeable being antibiotics that

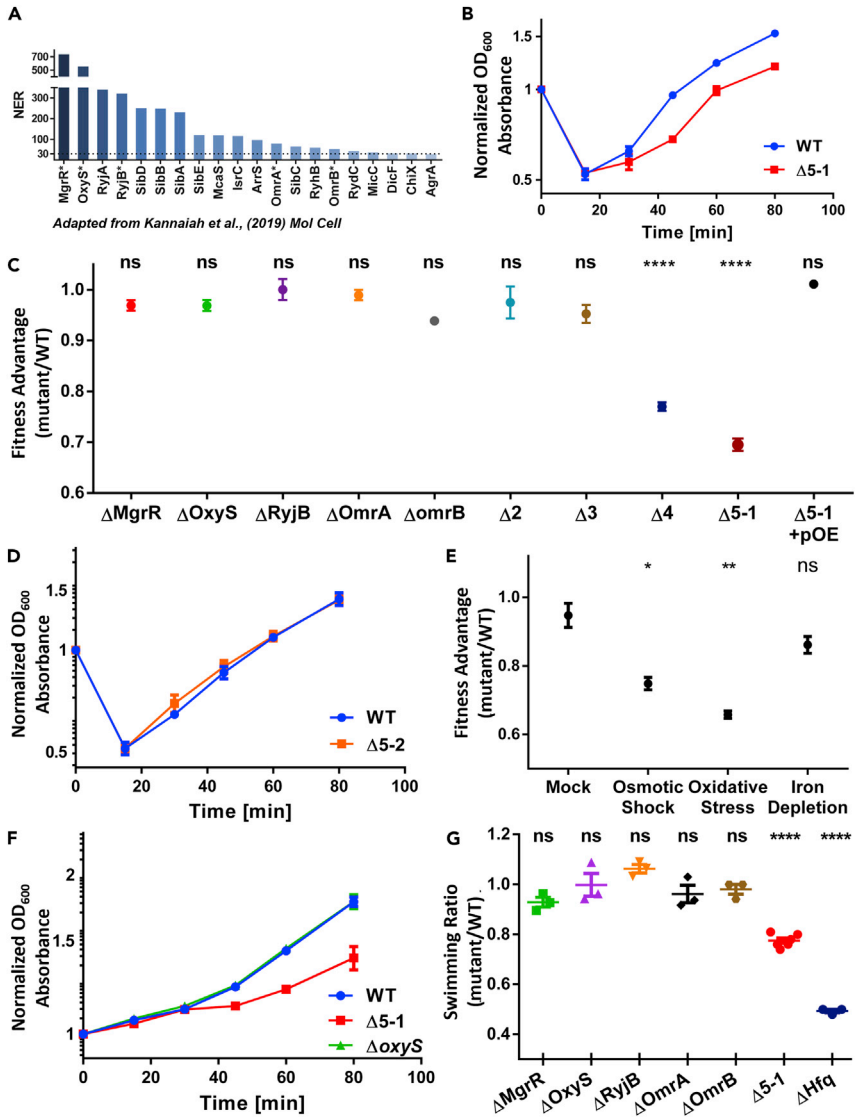

Figure 2. sRNAs act together to affect bacterial fitness during various stresses

(A) Top 20 sRNAs enriched at the poles. The NER (normalized enrichment ratio) index for each sRNA was calculated by dividing the polar fold enrichment after stress by the polar fold enrichment before the stress. sRNAs that were chosen for the sRNA-multi-KO strain are designated by an asterisk.

(B) Growth at high osmolarity of wild-type *E. coli* MG1655 (WT) strain compared with the sRNA-multi-KO strain deleted for five sRNAs, chosen unbiasedly as described in the text (Δ5-1). Cells were grown to mid-logarithmic phase and stressed by media replacement with LB supplemented with 20% sucrose. OD results were normalized to time 0, and data are represented as mean ± SEM from 3 independent experiments.

(C) Fitness analysis of WT cells (defined as 1), of cells deleted for each of the five sRNAs individually, or of cells with different sRNAs knockout combinations (Δ2, Δ3, Δ4, and Δ5-1), as well as of the Δ5-1 cells overexpressing the five sRNAs deleted in this strain (complementation, Δ5-1 + pOE), during osmotic shock. See Figures S5B and S5C for overexpression validation. Fitness was calculated as explained in the text, and data are represented as mean ± SEM from 3 independent experiments. Statistical analysis for the differences between mutants and WT was performed using *t test*. The calculated p value is ****<0.0001.

(D) Growth at high osmolarity of wild-type *E. coli* MG1655 compared with a strain deleted for five osmotic stress-related sRNAs KO (Δ5-2). Experimental details are as in (B). Data are represented as mean ± SEM from 3 independent experiments.

(E) Fitness analysis of the sRNA-multi-KO strain not stressed (mock) and subjected to osmotic shock, oxidative stress, or iron depletion, compared with WT (growth rate of WT in LB is defined as 1). Fitness was calculated as explained in the text based on the growth curves shown in Figure 2B (mock), Figure S5D (osmotic stress), Figure S5E (oxidative stress),

Figure 2. *Continued*

and Figure S5F (iron limitation). Statistical analysis was conducted as in (C). The calculated p values are * 0.0108 and ** 0.0023 for osmotic shock and oxidative stress, respectively. The bars show the SEM between three biological repeats.

(F) Growth during oxidative stress for WT, Δ*oxyS*, or sRNA-multi-KO strains. Cells were grown to mid-logarithmic phase and stressed by adding hydrogen peroxide to a final concentration of 1 mM. OD results were normalized to time 0, and data are represented as mean ± SEM from 3 independent experiments.

(G) Comparative swimming ability of WT (defined as 1), sRNA-multi-KO (Δ5), and single sRNA KO strains. Hfq deletion strain was used as a control for severe swimming ability defect. Statistical analysis was conducted as in Figure 2C. The calculated p value is ****<0.0001. The bars show the SEM between at least three biological repeats (n = 3, for Δ5-1 n = 6).

target the ribosome 30S and 50S subunits, as well as sRNAs whose level increase, e.g., OxyS, ArrS, and SgrS, or decrease, e.g., FnrS and Spot 42 (Spf), after treatments with all antibiotics. Interestingly, although we could not find a link between the sRNAs whose level increased in response to all antibiotics, FnrS and Spf, whose level decreased in response to all treatments, are both involved in carbon metabolism and they both have multiple targets whose expression they repress (Beisel and Storz, 2011; Durand and Storz, 2010).

Finally, we analyzed the changes in sRNAs expression under various infection-relevant conditions, extracted from the publicly available compendium of RNA-seq-based transcriptome analyses of *Salmonella Typhimurium* (Kröger et al., 2013) (Table S3). The results of this analysis (Figure S3) exhibited a similar trend to those observed for sRNAs in *E. coli*, that is, changes in the level of numerous sRNAs in response to each stress and certain sRNAs whose level changes, mainly increases, in response to many stresses.

Together these results suggest an orchestrated temporal changes in the expression of numerous sRNAs in response to many (though not all) changes in environmental conditions, which are in line with the existence of a polygenic plan for sRNA-mediated regulation.

Small RNAs act together to affect bacterial fitness during various stresses: proof of concept

In recent years it has become apparent that bacteria have adopted complex mechanisms for specific localization of macromolecules (Irastortza-Olaziregi and Amster-Choder, 2020; Rudner and Losick, 2010). Notably, enrichment of sRNAs before and, significantly more, after stress is confined to the cell poles (Kannaiah et al., 2019). The formation of polar hubs, where the concentration of sRNAs is higher than in the rest of the cell, thus enabling efficient regulation and production of optimal responses, is expected to be linked to similar localization patterns of sRNA-binding proteins (sRBPs). Indeed, Hfq, the main sRBP in *E. coli* and many other bacteria, which under nonstressed conditions distributes in the cell in a helical shape (Taghbalout et al., 2014), was recently shown to accumulate in the *E. coli* cell poles in response to high osmolarity and nitrogen starvation (Kannaiah et al., 2019; McQuail et al., 2020). These results, together with the dependence of sRNAs polar accumulation on Hfq during stress (Kannaiah et al., 2019), encouraged us to hypothesize that assembly of all network constituents at a certain location is advantageous for sRNA-mediated regulation.

To test this hypothesis, we asked whether interference with the polygenic plan for sRNAs, which takes into consideration that it is mainly executed at the cell poles and might be linked to Hfq, will reduce the ability of the cells to cope with stress. To this end, we created a list of the sRNAs that were detected at the poles (Kannaiah et al., 2019) and arranged them according to their normalized enrichment ratio (NER) index, which takes into consideration both the degree of their polar enrichment under nonstressed conditions and the increase in polar enrichment caused by the stress. The twenty most enriched sRNAs are shown in Figure 2A (NER>33). We then chose five sRNAs with a very high NER value, three from the very top of the list, which are intriguingly not related to osmotic stress (OxyS, MgrR, and RyjB), and two that exhibited the highest NER among osmolarity-related sRNAs (OmrA and OmrB) (the chosen sRNAs are marked by an asterisk in Figure 2A). For simplification, we chose sRNAs whose regulation by Hfq has been established and avoided the Sib antitoxin sRNAs that are quite enriched in this short list. These five sRNAs were deleted from the bacterial chromosome to create a multi-sRNA knockout strain ("Δ5-1"). Deletion of the five chosen sRNAs was confirmed by PCR and by whole-genome sequencing (Figure S4, see STAR Methods).

Notably, the Δ5-1 strain exhibited a disadvantage in growth compared to wild-type in high osmolarity (Figure 2B). Of note, the size of the wild-type and the Δ5-1 cells under high osmolarity was comparable (Figure S5A). As expected based on previous reports (Hobbs et al., 2010), knockout of each of the five

sRNA genes individually did not affect the ability of the bacteria to cope with stress, and the resulting strains grew like the wild-type strain (Figure 2C). Noteworthy, shown are fitness indexes that represent the growth of the mutant strain compared with the control wild-type strain (fitness analysis was conducted as reported previously (Mitchell et al., 2009); see STAR Methods). To see if the effect of the polar sRNA deletions is additive or cooperative, fitness analysis was conducted for strains harboring an increasing number of sRNA deletions in different combinations, all grown at high osmolarity. The representative results in Figure 2C show that no significant reduction in fitness was observed with two or three sRNA deletions. The results shown are for the strains deleted for the two stress-related sRNAs (OmrA and OmrB, Δ2) or for the three stress-unrelated sRNAs (MgrR, OxyS, and RyjB, Δ3). However, starting from deletion of four sRNA genes, fitness was reduced by ~20% and further reduced with five sRNA deletions (>25%). Ectopic expression of the five sRNAs, which have been deleted, from a plasmid (Δ5-1+pOE) in the Δ5-1 strain complemented the mutation and restored wild-type fitness. These results imply that the polarly enriched sRNAs may act in a cooperative, not necessarily synergistic, manner to cope with the stress.

An important control for our multiknockout strain (Δ5-1) was the construction of a strain deleted for five sRNAs, all known to be related to high osmolarity, MicA, MicC, MicF, OmrA, and OmrB, termed Δ5-2. Interestingly, none of these osmotic-stress-related sRNAs appeared at the very top of the NER list, which was obtained from cells exposed to high osmolarity, although three are in the list of the top 20 (Figure 2A). No growth rate defect was observed with this strain compared with wild-type (Figure 2D). Of note, growth and fitness were not monitored in a strain deleted for *hfq* because, in addition to its role as sRNA-mRNA matchmaker, Hfq plays important roles in translation, through its binding to rRNA and tRNA, and in DNA compaction, via its binding to the chromosome, explaining the pleiotropic effect of the Δ*hfq* mutant (dos Santos et al., 2019).

Because three of the five sRNAs that were deleted in the Δ5-1 strain are not related to osmotic stress, and because all five deleted sRNAs were shown to be enriched at the poles also under nonstress conditions (Kannaiah et al., 2019), we examined whether this set of deletions affects bacterial growth in other stress conditions: oxidative stress and iron limitation. The results in Figure 2E show that the fitness of this strain was significantly reduced by more than 30% in oxidative stress and by 14%, although not significantly, in a low-iron condition. To test whether the former result is due to the fact that OxyS, the main regulator that protects cells against oxidative damage (Altuvia et al., 1997), was one of the sRNAs deleted in this strain, we compared the effect of deleting only the *oxyS* gene (ΔOxyS) with that of deleting all five sRNA genes, including *oxyS* (Δ5-1), on growth of bacterial cells exposed to oxidative stress. The results in Figure 2F show that the Δ*oxyS* strain did not have any observed growth defect and grew just like the wild-type (green and blue lines overlap), whereas the Δ5-1 strain (red line) exhibited a significant reduction in growth under this condition.

Taking into consideration that deletion of five polarly enriched sRNAs affects bacterial ability to cope with different conditions, we decided to compare the motility of the Δ5-1 strain to that of the wild-type strain by comparing their ability to swim in soft agar plates. We chose to test motility, an important feature of bacteria that enables them to change their environmental niche and lifestyle, because it has been shown to be directly and indirectly modulated by a surprisingly large number of sRNAs (Mika and Hengge, 2013) and for the simplicity of assaying it. The results in Figure 2G show that the swimming ability of the Δ5-1 strain was reduced by more than 20% compared with wild-type (see STAR Methods for motility assay). An *hfq* deletion strain, previously shown to have reduced swimming ability (Fernandez et al., 2016; Simonsen et al., 2011), served as a control. In line with previously reported results (Bak et al., 2015), no single sRNA deletion conferred a significant change on the bacterial swimming ability (Figure 2G), in contrast to the Δ5-1 strain and the Δ*hfq* mutant, the latter known to have severe pleiotropic defects (see above).

Together, our results expose the need for a collective action of sRNAs to cope with environmental changes and are in line with the polygenic plan. The observed polar accumulation of sRNAs before and after stress (Kannaiah et al., 2019) and the effect of deleting several sRNAs that are enriched in the poles on bacterial ability to cope with different stresses reinforce the notion that the poles are hubs that enable efficient sRNA-mediated regulation. Whether the selected sRNAs are part of a core sRNA genes and who are the peripheral genes in the polygenic program requires further research utilizing high-throughput methods.

DISCUSSION

The evolutionary benefits arising from regulatory plans that involve many genes – polygenic plans – are obvious because they add additional layers of control to gene expression and increase the power and

robustness of the underlying mechanisms. The feasibility of the polygenic view has been considered thus far for eukaryotic organisms, based on results obtained by whole-genome and transcriptome sequencing (Barton et al., 2017) (Boyle et al., 2017), but not for prokaryotes. Previously published data suggested that bacterial response to stress involves numerous sRNAs (Kannaiah et al., 2019), suggesting that this view is relevant also for prokaryotes. Here, we provided several types of evidence for the existence of a polygenic plan for regulation by sRNAs. We show that the level of numerous genes changes in response to various environmental conditions, most of them not known to respond to these conditions, and that the ability to cope with different conditions can be partially compromised by deleting five sRNAs that are highly enriched in the cell poles, where sRNAs and their chaperon Hfq gather upon stress. Together, our results imply that polygenic regulatory plans are relevant for bacteria as well. Further work is required to elucidate the mechanism(s) underlying such plans in all cell types.

The five deleted sRNAs, which were chosen subjectively, based on their preferential enrichment at the poles of nonstressed cells, in addition to their dramatic increase at the poles upon osmotic stress, cannot be classified yet as core genes for a global plan, although at least some of them might serve as such in less inclusive plans. Our results suggest that the core RNA for environmental stresses differs from those for antibiotic treatments. Also, the ability of these five sRNAs to regulate their target mRNAs is not necessarily the reason for their effect on the ability of the bacterial cells to deal with various situations, as they might act as sponges for other sRNAs, competitors by occupying Hfq, Hfq ushers and so on. Importantly, while our study focuses specifically on a polygenic plan for sRNA-mediated regulation, there is no reason to think that this phenomenon does not extend beyond this type of regulation. Having said that, it should not be too surprising if the plan for sRNAs differs from the plan(s) for other RNAs because their posttranscriptional fate completely differs from that of other RNAs, as sRNAs are not bound by ribosomes, rather they are bound by dedicated chaperons.

The many sRNAs, whose level change in response to each stimulus or that accumulate at the poles upon osmotic stress, can be divided into several categories depending on the sRBP they bind (Hfq ProQ, CsrA, or not known), their mechanism of action (base-pairing with other RNA, binding to proteins or being part of toxin-antitoxin systems), or the transcription factor that is responsible for their expression. Although all these sRNAs are not very likely to be evolutionarily related, they belong to a limited number of categories, the members of each are evolutionarily conserved, which seemingly adapted the same strategy during evolution. In our low-throughput experiments (Figures 1A, 1B, and 2), we monitored or deleted only sRNAs that bind to Hfq, which is the primary sRBP in *E. coli*, and avoided those that are part of toxin-antitoxin systems. Hence, it remains to be seen whether there is a global plan for forming a sRNA network linking members of all categories and for bringing all of them to the poles or there are several parallel or connected plans.

The consequences of ineffective regulatory networks, which are intended to cope with environmental changes, in unicellular organisms with short generation time might be as severe as cell death and, eventually, population extinction. Farther to this, the importance of sRNA-associated regulatory networks for coping with and surviving in ever-changing and challenging environments seems to be manifested in their multidimensionality and complexity. Several components contribute to the complexity of the regulatory circuits that involve sRNAs, among them: *i)* Expression of the various sRNAs is controlled by different transcription factors, each responding to one or several environmental signals. *ii)* Several sRBPs facilitate sRNA-mRNA base-pairing, the most studied being Hfq, ProQ, and CsrA (Quendera et al., 2020). Although each seems to bind to a set of unique sRNAs, many sRNAs bind to more than one sRBP, indicating overlapping roles and competition between the sRBPs. Competition among mRNA targets over the same sRBP also plays a role in the regulatory outcome (Faigenbaum-Romm et al., 2020). *iii)* Different environmental conditions induce different, sometimes opposing, changes in the expression of both sRNAs and mRNAs. *iv)* Rewiring, i.e., changing the mRNA partner/s of a given sRNA, due to environmental changes, adds to the complexity (Holmqvist et al., 2016, 2018; Melamed et al., 2016, 2020), e.g., the number of RyhB targets increases from only 5 mRNAs in the logarithmic phase to 178 mRNAs upon iron limitation (data adapted from the study by Melamed et al., 2016). This multilayer complexity, which requires high-level dynamics, creates an extremely tangled polygenic net. Elucidating the mechanisms underlying this complex plan requires additional studies by high-throughput approaches.

To implement an efficient and robust polygenic program for sRNA-mediated regulation, the temporal level of the sRNAs must be tightly controlled and the cellular location of all components, including sRNAs, mRNAs, and sRBPs, must be coordinated. Mechanisms that might be involved in achieving this high-level

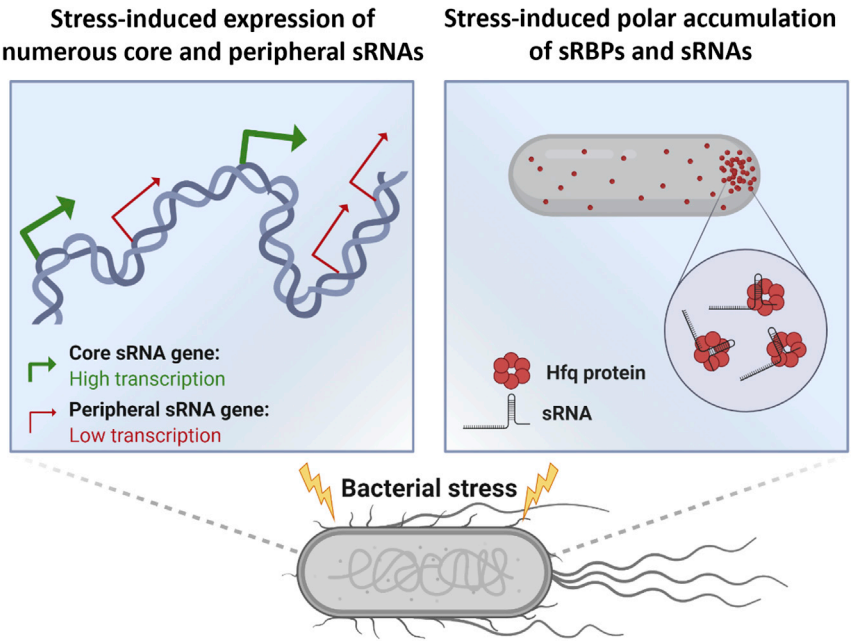

Figure 3. A scheme describing putative aspects of the polygenic and spatial plans for sRNA-mediated regulation

A combined mechanism relying on stress-induced expression of a collection of core and peripheral sRNA genes (left panel) and on accumulation of the sRNAs and their chaperon Hfq at the cell pole (right panel) is suggested to underlie regulation by sRNAs. The identity and the number of core and peripheral sRNA genes that are expressed are expected to vary depending on the stress, the transcription plan, the sRBPs involved, and the level of transcriptional plasticity (see discussion). Illustration was created with BioRender.com.

spatiotemporal intricacy are as follows: *i)* High-level expression of core sRNA genes that are common to many environmental changes/stresses and lower level of sets of peripheral genes that confer specificity (Figure 3, left panel). The role of the core sRNAs might vary between recruitment of the sRBPs to supplying a scaffold for the network or acting as sponges for other sRNAs. *ii)* Transcriptional plasticity of the entire family of sRNAs may underlie cellular adaptation to stresses. It has been shown that cellular adaptation to novel challenges is characterized by plasticity, whereby different solutions are possible (Stern et al., 2007). Hence, different combinations of core and peripheral sRNAs, expressed in varying levels, may offer different solutions to a given stress. *iii)* Increasing the cellular arsenal to ensure redundancy and guarantee sRNAs availability upon extreme environmental hazards. *iv)* Increasing the effective concentration of the different players, RNAs and sRBPs, by concentrating them in a certain domain, the bacterial poles in this case. This gathering at a defined location should facilitate their interaction and enable cross talk (Figure 3, right panel). Achieving local high concentration and proximity of the RNA and protein constituents that are needed for polygenic regulation might be made possible by reliance on liquid-liquid phase separation (LLPS) (Boeynaems et al., 2018; Langdon and Gladfelter, 2018).

Summarily, existing data on the complexity of sRNA-regulated networks, examined within the context of both established and novel concepts such as functional redundancy, LLPS, and plasticity, suggest ways in which the novel paradigm of polygenic regulation in bacteria, which is likely to play a central role in adaptations, may be implemented.

Limitations of the study

This study provides a proof of concept for the existence of a sRNA polygenic plan for coping with environmental cues. Whether the sRNAs that we deleted are core global components of this plan or they are dedicated to the various stresses that we applied, as well as the identity of the peripheral genes in the polygenic program, requires further research utilizing high-throughput methods.

STAR★METHODS

Detailed methods are provided in the online version of this paper and include the following:

SUPPLEMENTAL INFORMATION

Supplemental information can be found online at https://doi.org/10.1016/j.isci.2021.103096.

ACKNOWLEDGMENTS

We acknowledge Gisela Storz for the gift of single-sRNA knockout strains. We appreciate fruitful discussions with members of O.A.-C. laboratory and with Hanah Margalit. We thank Meshi Barsheshet for help with computational analyses. This research was supported by the Israel Science Foundation (ISF) founded by the Israel Academy of Sciences and Humanities (1274/19) and the Deutsch-Israeli Project Cooperation (DIP) (AM 441/1-1 SO 568/1-1). O.G. is funded by a PhD fellowship from the Israel Ministry of Science and Technology (19400201).

AUTHOR CONTRIBUTIONS

O.G. designed the study, conducted the experiments, and analyzed data. R.B. isolated the clinical *E. coli* strain. J.L. and R.B. generated the RNA-Seq data for the clinical *E. coli* strain after exposure to antibiotics. O.A.-C. provided advice and contributed to experimental design. O.A.-C. and O.G. wrote manuscript.

DECLARATION OF INTEREST

The authors declare no competing interests.

Received: November 16, 2020
Revised: February 18, 2021
Accepted: September 2, 2021
Published: October 22, 2021

REFERENCES

Abeel, T., Van Parys, T., Saeys, Y., Galagan, J., and Van De Peer, Y. (2012). GenomeView: a next-generation genome browser. Nucleic Acids Res. *40*, 1–10.

Altuvia, S., Weinstein-fischer, D., Zhang, A., Postow, L., and Storz, G. (1997). A small , stable RNA induced by oxidative Stress : role as a pleiotropic regulator and antimutator. Cell *90*, 43–53.

Amster-choder, O. (2011). The compartmentalized vessel. Cell. Logist. *1*, 77–81.

Bak, G., Lee, J., Suk, S., Kim, D., Lee, J.Y., Kim, K.S., Choi, B.S., and Lee, Y. (2015). Identification of novel sRNAs involved in biofilm formation, motility, and fimbriae formation in Escherichia coli. Sci. Rep. *5*, 1–19.

Barton, N.H., Etheridge, A.M., and Véber, A. (2017). The infinitesimal model: definition, derivation, and implications. Theor. Popul. Biol. *118*, 50–73.

Basyuk, E., Rage, F., and Bertrand, E. (2020). RNA transport from transcription to localized translation: a single molecule perspective. RNA Biol. *18*, 1221–1237.

Beisel, C.L., and Storz, G. (2011). The base-pairing RNA Spot 42 participates in a multioutput feedforward loop to help enact catabolite repression in Escherichia coli. Mol. Cell *41*, 286–297.

Bergthorsson, U., and Ochman, H. (1998). Distribution of chromosome length variation in natural isolates of Escherichia coli. Mol. Biol. Evol. *15*, 6–16.

Bhattacharyya, R.P., Bandyopadhyay, N., Ma, P., Son, S.S., Liu, J., He, L.L., Wu, L., Khafizov, R., Boykin, R., Cerqueira, G.C., et al. (2019). Simultaneous detection of genotype and phenotype enables rapid and accurate antibiotic susceptibility determination. Nat. Med. *25*, 1858–1864.

Boeynaems, S., Alberti, S., Fawzi, N.L., Mittag, T., Polymenidou, M., Rousseau, F., Schymkowitz, J., Shorter, J., Wolozin, B., Van Den Bosch, L., et al. (2018). Protein phase separation: a new phase in cell biology. Trends Cell Biol. *28*, 420–435.

Boyle, E.A., Li, Y.I., and Pritchard, J.K. (2017). An expanded view of complex traits: from polygenic to omnigenic. Cell *169*, 1177–1186.

Chen, Z., Wang, Y., Li, Y., Li, Y., Fu, N., Ye, J., and Zhang, H. (2012). Esre: a novel essential non-coding RNA in Escherichia coli. FEBS Lett. *586*, 1195–1200.

Cherepanov, P.P., and Wackernagel, W. (1995). Gene disruption in Escherichia coli: TcR and KmR cassettes with the option of Flp-catalyzed excision of the antibiotic-resistance determinant. Gene *158*, 9–14.

Chin, A., and Lécuyer, E. (2017). RNA localization: making its way to the center stage. Biochim. Biophys. Acta *1861*, 2956–2970.

Durand, S., and Storz, G. (2010). Reprogramming of anaerobic metabolism by the FnrS small RNA. Mol. Microbiol. *75*, 1215–1231.

Faigenbaum-romm, R., Reich, A., Gatt, Y.E., Barsheshet, M., Argaman, L., and Margalit, H. (2020). Hierarchy in hfq chaperon occupancy of small RNA targets plays a major role in their regulation article hierarchy in hfq chaperon occupancy of small RNA targets plays a major role in their regulation. Cell Rep. *30*, 3127–3138.e6..

Felden, B., and Cattoira, V. (2018). Bacterial adaptation to antibiotics through regulatory RNAs. Antimicrob. Agents Chemother. *62*, 1–11.

Fernandez, L., Breidenstein, E.B.M., Taylor, P.K., Bains, M., De La Fuente-Nunez, C., Fang, Y., Foster, L.J., and Hancock, R.E.W. (2016). Interconnection of post-transcriptional regulation: the RNA-binding protein Hfq is a novel target of the Lon protease in Pseudomonas aeruginosa. Sci. Rep. *6*, 1–11.

Fisher, R.A. (2019). The causes of human variability. Int. J. Epidemiol. *48*, 7–10.

Gripenland, J., Netterling, S., Loh, E., Tiensuu, T., Toledo-Arana, A., and Johansson, J. (2010). RNAs: regulators of bacterial virulence. Nat. Rev. Microbiol. *8*, 857–866.

Grove, J., Ripke, S., Als, T.D., Mattheisen, M., Walters, R.K., Won, H., Pallesen, J., Agerbo, E., Andreassen, O.A., Anney, R., et al. (2019). Identification of common genetic risk variants for autism spectrum disorder. Nat. Genet. *51*, 431–444.

Guillier, M., and Gottesman, S. (2006). Remodelling of the Escherichia coli outer membrane by two small regulatory RNAs. Mol. Microbiol. *59*, 231–247.

Hayes, E.T., Wilks, J.C., Sanfilippo, P., Yohannes, E., Tate, D.P., Jones, B.D., Radmacher, M.D., BonDurant, S.S., and Slonczewski, J.L. (2006). Oxygen limitation modulates pH regulation of catabolism and hydrogenases, multidrug transporters, and envelope composition in Escherichia coli K-12. BMC Microbiol. *6*, 1–18.

Hillenmeyer, M.E., Fung, E., Wildenhain, J., Pierce, S.E., Hoon, S., Lee, W., Proctor, M., St.Onge, R.P., Tyers, M., Koller, D., et al. (2008). The chemical genomic portrait of yeast: uncovering a phenotype for all genes. Science *320*, 362–365.

Hobbs, E.C., Astarita, J.L., and Storz, G. (2010). Small RNAs and small proteins involved in resistance to cell envelope stress and acid shock in Escherichia coli: analysis of a bar-coded mutant collection. J. Bacteriol. *192*, 59–67.

Holmqvist, E., and Wagner, E.G.H. (2017). Impact of bacterial sRNAs in stress responses. Biochem. Soc. Trans. *45*, 1203–1212.

Holmqvist, E., Wright, P.R., Li, L., Bischler, T., Barquist, L., Reinhardt, R., Backofen, R., and Vogel, J. (2016). Global RNA recognition patterns of post-transcriptional regulators Hfq and CsrA revealed by UV crosslinking in vivo. EMBO J. *35*, 991–1011.

Holmqvist, E., Li, L., Bischler, T., Barquist, L., and Vogel, J. (2018). Global maps of ProQ binding in vivo reveal target recognition via RNA structure and stability control at mRNA 3′ ends. Mol. Cell *70*, 971–982.e6.

Hör, J., Matera, G., Vogel, J., Gottesman, S., and Storz, G. (2020). Trans-acting small RNAs and their effects on gene expression in Escherichia coli and Salmonella enterica. EcoSal Plus *9*.

Irastortza-Olaziregi, M., and Amster-Choder, O. (2020). RNA localization in prokaryotes: where, when, how, and why. Wiley Interdiscip. Rev. RNA *12*, 1–27.

Jacob, F., and Monod, J. (1961). Genetic regulatory mechanisms in the synthesis of proteins. J. Mol. Biol. *3*, 318–356.

Jansen, I.E., Savage, J.E., Watanabe, K., Bryois, J., Williams, D.M., Steinberg, S., Sealock, J., Karlsson, I.K., Hägg, S., Athanasiu, L., et al. (2019). Genome-wide meta-analysis identifies new loci and functional pathways influencing Alzheimer's disease risk. Nat. Genet. *51*, 404–413.

Kannaiah, S., Livny, J., and Amster-Choder, O. (2019). Spatiotemporal organization of the E. coli transcriptome: translation independence and engagement in regulation. Mol. Cell *76*, 574–589.e7.

Kröger, C., Colgan, A., Srikumar, S., Händler, K., Sivasankaran, S.K., Hammarlöf, D.L., Canals, R., Grissom, J.E., Conway, T., Hokamp, K., et al. (2013). An infection-relevant transcriptomic compendium for salmonella enterica serovar typhimurium. Cell Host Microbe *14*, 683–695.

Langdon, E.M., and Gladfelter, A.S. (2018). A new lens for RNA localization: liquid-liquid phase separation. Annu. Rev. Microbiol. *72*, 255–271.

Li, H., and Durbin, R. (2009). Fast and accurate short read alignment with Burrows-Wheeler transform. Bioinformatics *25*, 1754–1760.

Love, M.I., Huber, W., and Anders, S. (2014). Moderated estimation of fold change and dispersion for RNA-seq data with DESeq2. Genome Biol *15*, 1–21.

Mandin, P., and Gottesman, S. (2010). Integrating anaerobic/aerobic sensing and the general stress response through the ArcZ small RNA. EMBO J. *29*, 3094–3107.

Masse, E., Vanderpool, C.K., and Gottesman, S. (2005). Effect of RyhB small RNA on global iron use in Escherichia coli. J. Bacteriol. *187*, 6962–6971.

McQuail, J., Switzer, A., Burchell, L., and Wigneshweraraj, S. (2020). The RNA-binding protein Hfq assembles into foci-like structures in nitrogen starved Escherichia coli. J. Biol. Chem. *295*, 12355–12367.

Melamed, S., Peer, A., Faigenbaum-Romm, R., Gatt, Y.E., Reiss, N., Bar, A., Altuvia, Y., Argaman, L., and Margalit, H. (2016). Global mapping of small RNA-target interactions in bacteria. Mol. Cell *63*, 884–897.

Melamed, S., Adams, P.P., Zhang, A., Zhang, H., and Storz, G. (2020). RNA-RNA interactomes of ProQ and hfq reveal overlapping and competing roles. Mol. Cell *77*, 411–425.e7.

Mika, F., and Hengge, R. (2013). Small regulatory RNAs in the control of motility and biofilm formation in E. Coli and Salmonella. Int. J. Mol. Sci. *14*, 4560–4579.

Mitchell, A., Romano, G.H., Groisman, B., Yona, A., Dekel, E., Kupiec, M., Dahan, O., and Pilpel, Y. (2009). Adaptive prediction of environmental changes by microorganisms. Nature *460*, 220–224.

Moon, K., and Gottesman, S. (2009). A PhoQ/P-regulated small RNA regulates sensitivity of Escherichia coli to antimicrobial peptides. Mol. Microbiol. *74*, 1314–1330.

Nevo-Dinur, K., Nussbaum-Shochat, A., Ben-Yehuda, S., and Amster-Choder, O. (2011). Translation-independent localization of mRNA in E. coli. Science *331*, 1081–1084.

Papenfort, K., and Vogel, J. (2010). Regulatory RNA in bacterial pathogens. Cell Host Microbe *8*, 116–127.

Quendera, A.P., Seixas, A.F., dos Santos, R.F., Santos, I., Silva, J.P.N., Arraiano, C.M., and Andrade, J.M. (2020). RNA-binding proteins driving the regulatory activity of small non-coding RNAs in bacteria. Front. Mol. Biosci. *7*, 1–9.

Quereda, J.J., and Cossart, P. (2017). Regulating bacterial virulence with RNA. Annu. Rev. Microbiol. *71*, 263–280.

Ramani, A.K., Chuluunbaatar, T., Verster, A.J., Na, H., Vu, V., Pelte, N., Wannissorn, N., Jiao, A., and Fraser, A.G. (2012). The majority of animal genes are required for wild-type fitness. Cell *148*, 792–802.

Rudner, D.Z., and Losick, R. (2010). Protein subcellular localization in bacteria. Cold Spring Harb. Perspect. Biol. *2*, a000307.

dos Santos, R.F., Arraiano, C.M., and Andrade, J.M. (2019). New molecular interactions broaden the functions of the RNA chaperone Hfq. Curr. Genet. *65*, 1313–1319.

Shishkin, A.A., Giannoukos, G., Kucukural, A., Ciulla, D., Busby, M., Surka, C., Chen, J., Bhattacharyya, R.P., Rudy, R.F., Patel, M.M., et al. (2015). Simultaneous generation of many RNA-seq libraries in a single reaction. Nat. Methods *12*, 323–325.

Simonsen, K.T., Nielsen, G., Bjerrum, J.V., Kruse, T., Kallipolitis, B.H., and Møller-Jensen, J. (2011). A role for the RNA chaperone Hfq in controlling Adherent-invasive Escherichia coli colonization and virulence. PLoS One *6*, e16387.

Stern, S., Dror, T., Stolovicki, E., Brenner, N., and Braun, E. (2007). Genome-wide transcriptional plasticity underlies cellular adaptation to novel challenge. Mol. Syst. Biol. *3*, 1–10.

Storz, G., Vogel, J., and Wassarman, K.M. (2011). Regulation by small RNAs in bacteria: expanding frontiers. Mol. Cell *43*, 880–891.

Taghbalout, A., Yang, Q., and Arluison, V. (2014). The Escherichia coli RNA processing and degradation machinery is compartmentalized within an organized cellular network. Biochem. J. *458*, 11–22.

Vanderpool, C.K., and Gottesman, S. (2004). Involvement of a novel transcriptional activator and small RNA in post-transcriptional regulation of the glucose phosphoenolpyruvate phosphotransferase system. Mol. Microbiol. *54*, 1076–1089.

Vogel, J., and Papenfort, K. (2006). Small non-coding RNAs and the bacterial outer membrane. Curr. Opin. Microbiol. *9*, 605–611.

Westermann, A.J. (2018). Regulatory RNAs in virulence and host-microbe interactions. Microbiol. Spectr. *6*, 305–337.

Wiegand, I., Hilpert, K., and Hancock, R.E.W. (2008). Agar and broth dilution methods to determine the minimal inhibitory concentration (MIC) of antimicrobial substances. Nat. Protoc. *3*, 163–175.

Winzeler, E.A., Shoemaker, D.D., Astromoff, A., Liang, H., Andre, B., Bangham, R., Benito, R., Boeke, J.D., Bussey, H., Chu, A.M., et al. (1999). Analysis linked references are available on JSTOR for this article : functional characterization of the S . Cerevisiae genome by gene deletion and parallel analysis. Science *285*, 901–906.

Xue, A., Wu, Y., Zhu, Z., Zhang, F., Kemper, K.E., Zheng, Z., Yengo, L., Lloyd-Jones, L.R., Sidorenko, J., Wu, Y., et al. (2018). Genome-wide association analyses identify 143 risk variants and putative regulatory mechanisms for type 2 diabetes. Nat. Commun. *9*, 2941.

STAR★METHODS

KEY RESOURCES TABLE

REAGENT or RESOURCE	SOURCE	IDENTIFIER
Bacterial and virus strains		
Escherichia coli K-12 MG1655 (F-, *λ-, rph-1*)	General lab strain	MG1655
Escherichia coli K-12 MG1655 *mgrR::Kan*	(Hobbs et al., 2010)	Δ*mgrR*
Escherichia coli K-12 MG1655 *oxyS::Kan*	(Hobbs et al., 2010)	Δ*oxyS*
Escherichia coli K-12 MG1655 *ryjB::Kan*	(Hobbs et al., 2010)	Δ*ryjB*
Escherichia coli K-12 MG1655 *omrA::Kan*	(Hobbs et al., 2010)	Δ*omrA*
Escherichia coli K-12 MG1655 *omrB::Kan*	(Hobbs et al., 2010)	Δ*omrB*
Escherichia coli K-12 MG1655 *omrAB::Kan*	(Hobbs et al., 2010)	Δ2
Escherichia coli K-12 MG1655 Δ*mgrR; omrAB::Kan*	This Paper	Δ3
Escherichia coli K-12 MG1655 Δ*mgrR;* Δ*oxyS;* Δ*ryjB; omrA::Kan*	This Paper	Δ4
Escherichia coli K-12 MG1655 Δ*mgrR;* Δ*oxyS;* Δ*ryjB; omrAB::Kan*	This Paper	Δ5-1
Escherichia coli K-12 MG1655 *micA::Kan*	(Hobbs et al., 2010)	Δ*micA*
Escherichia coli K-12 MG1655 *micC::Kan*	(Hobbs et al., 2010)	Δ*micC*
Escherichia coli K-12 MG1655 *micF::Kan*	(Hobbs et al., 2010)	Δ*micF*
Escherichia coli K-12 MG1655 Δ*micF;* Δ*micA;* Δ*omrA;* Δ*omrB;* Δ*micC::kan*	This Paper	Δ5-2
Escherichia coli K-12 MG1655 Hfq::*Kan*	(Kannaiah et al., 2019)	Δ*hfq*
Escherichia coli RB001	(Bhattacharyya et al., 2019)	Clinical isolate
Chemicals, peptides, and recombinant proteins		
TriReagent Solution	Sigma-Aldrich	Cat#T9424
Hydrogen Peroxide Solution	Sigma-Aldrich	Cat#216763
2,2′-Bipyridyl	Sigma-Aldrich	Cat#D216305
FastAP Thermosensitive Alkaline Phosphatase (1 U/μL)	Thermo Fisher	Cat#EF0652
TURBO DNase (2 U/μL)	Thermo Fisher	Cat#AM2239
SUPERase Rnase inhibitor (20U/ul)	Life Technologies	Cat#AM2694
Ampure RNAClean XP beads	Beckman Coulter	Cat#A63881
Ligase,T4 RNA 1, ssRNA/3x 5000U (1PK)	NEB	Cat#M0437M
dNTP Mix (200415)	Agilent	Cat#200415
Exonuclease I Enzyme	NEB	Cat#M0293L
Agencourt Ampure XP DNA beads	Beckman Coulter	Cat#A63881
Buffer RLT	Qiagen	Cat#79216
Azithromycin	Sigma-Aldrich	Cat #75199
Ceftriaxone	Sigma-Aldrich	Cat# C5793
Chloramphenicol	Sigma-Aldrich	Cat #C0378
Ciprofloxacin	Sigma-Aldrich	Cat #17850
Doxycycline	Sigma-Aldrich	Cat #D9891
Gentamicin	Sigma-Aldrich	Cat #G1914
Nitrofurantoin	Sigma-Aldrich	Cat #N7878
Novobiocin	Sigma-Aldrich	Cat #N1628

(*Continued on next page*)

Continued

REAGENT or RESOURCE	SOURCE	IDENTIFIER
Phleomycin	Sigma-Aldrich	Cat #P9564
Sulfamethoxazole	Sigma-Aldrich	Cat #S7507
Trimethoprim	Sigma-Aldrich	Cat #T7883
Critical commercial assays		
iTaq Universal SYBER Green Supermix	Bio-Rad	Cat#1725121
Direct-zol RNA Miniprep Kit	Zymo Research	Cat#R2060
qScript cDNA synthesis Kit	Quanta bio	Cat#95047
Qubit RNA HS Assay Kit	Thermo Scientific	Cat#Q32852
Turbo DNA-free Kit	Ambion	Cat#AM1907
NucleoSpin Plasmid EasyPure Kit	Machery-Nagel	Cat#740727
NucleoSpin Gel and PCR clean-up Kit	Machery-Nagel	Cat#740609
Ribo-Zero rRNA Removal Kit	Illumina	Cat#MRZB12424
SMARTScribe Reverse Transcriptase	Takara Bio	Cat#639538
High Sensitivity RNA Screentape reagent	Agilent	Cat#5067-5580
RNA Clean & Concentrator Kit	Zymo Research	Cat#R1013
AccuPrime Taq HiFi Kit	Life Technologies	Cat#12346094
High Sensitivity D1000 Screentape reagent	Agilent	Cat#5067-1511
Qubit dsDNA High Sensitivity Kit	Life Technologies	Cat#Q32854
Wizard Genomic DNA Purification Kit	Promega	Cat#A1120
Deposited data		
Log, stationery, and Iron limitation data	(Melamed et al., 2016)	Database: E-MTAB-3910
RB001 antibiotic challenges data	This paper	Database: PRJNA707564
MG1655 High osmolarity RNA-seq data	(Kannaiah et al., 2019)	Database: SRA:PRJNA517279
Oligonucleotides		
Real-time PCR: *rybB* Forward-GCCACTGCTTTTCTTTGATGTCCReverse-ACAAAAAACCCATCAACC	(Kannaiah et al., 2019)	N/A
Real-time PCR: *arcZ* Forward-GTGCGGCCTGAAAAACAGReverse-AAAAAATGACCCCGGCTAG	(Kannaiah et al., 2019)	N/A
Real-time PCR: *omrA* Forward-CCCAGAGGTATTGATTGGTGAGReverse-CGCAGGTTGGTGCAAGAGAC	(Kannaiah et al., 2019)	N/A
Real-time PCR: *omrB* Forward-CCCAGAGGTATTGATAGGTGAAGReverse-GCATCTGCGCAGGCTGG	(Kannaiah et al., 2019)	N/A
Real-time PCR: *micA* Forward-AAGACGCGCATTTGTTATCATCReverse-CACTCGTGAGTG GCC	Hanah Margalit Lab	N/A
Real-time PCR: *micC* Forward-TCTGTTGGGCCATTGCATReverse-GACGACTGTTCGGGCTTG	This paper	N/A
Real-time PCR: *oxyS* Forward-AACCCTTGAAGTCACTGCCCReverse-GGAGATCCGCAAAAGTTCACG	This paper	N/A

(*Continued on next page*)

Continued

REAGENT or RESOURCE	SOURCE	IDENTIFIER
Real-time PCR: *mgrR* Forward-GAAAATGCCTGTTAGCGTAAAAGReverse-CGGCGGTGAATGCTT	Hanah Margalit Lab	N/A
Real-time PCR: *sgrS* Forward-GCTGGTTGCGTTGGTTAAGReverse-GCAGGCAAGTCAACTTTCAG	This paper	N/A
Real-time PCR: *gadY* Forward-ACTGAGAGCACAAAGTTTCCReverse-AAAAAAAACCCGGCATAGGG	This paper	N/A
Real-time PCR: *ryjB* Forward-TCATCCGTCGTTGACTCCATReverse-CTGCCGCCTTCGTCAAA	This paper	N/A
Recombinant DNA		
pCP20	(Cherepanov and Wackernagel, 1995)	N/A
pQE80L	Qiagen	CAT#32943
pQE80L-sRNAsOE	This paper	pOE
Software and algorithms		
DESeq2	(Love et al., 2014)	https://bioconductor.orgpackages/release/bioc/htmlDESeq2.html
R	The R foundation	http://www.r-project.org/
NIS Elements Advanced Research (AR) version 4.5	Nikon	N/A
GraphPad Prism v6	GraphPad	https://www.graphpad.com/scientific-software/prism/
Image Lab v6.0.1	Bio-Rad	http://www.bio-rad.com/en-il/product/image-lab-software

RESOURCE AVAILABILITY

Lead contact

Further information and requests should be directed to the lead contact, Orna Amster-Choder (ornaam@ekmd.huji.ac.il).

Materials availability

Bacterial strains will be made available upon request.

Data and code availability

- The RNA-seq data for *E. coli* under antibiotic challenges generated in this study is publicly available as of the date of publication. Accession numbers are listed in the key resources table.
- This paper does not report new or original code.
- The raw data for the manuscript is available on request from the lead contact Prof. Orna Amster-Choder (ornaam@ekmd.huji.ac.il).

EXPERIMENTAL MODEL AND SUBJECT DETAILS

Bacterial strains and growth conditions

All bacterial strains used in this study are listed in the Key resources table. Unless otherwise stated, overnight cultures were grown at 30°C in LB and diluted 1:100 into LB supplemented with the appropriate antibiotics at the following concentrations: kanamycin (30 μg/ml) and/or ampicillin (200 μg/ml). If not indicated that the gene was overexpressed, it was expressed from its native gene promoter and locus in the

chromosome. Expression from plasmids was induced by 0.1 mM IPTG. To induce envelope stress, cells were grown to mid-logarithmic phase, pelleted and resuspended in fresh LB supplemented with 20% sucrose and further grown for the desired time. To induce oxidative stress and iron limitation, 1 mM hydrogen peroxide and 0.2 mM 2,20-dipyridyl, respectively, were added to mid-logarithmic phase cells.

METHOD DETAILS

Multiple sRNA KO strain construction

The *oxyS* deletion was transferred to the Δ*mgrR* strain by P1 transduction. The kanamycin resistance gene was removed by transforming with pCP20 and selecting on LB plates containing ampicillin incubated at 30°C. The pCP20 plasmid was later cured by growing the cells at 42°C. All other deletions were introduced by the same procedure to the different knockout strains.

Genome sequencing and analysis

Genomic DNA of Δ5-1 was isolated using Wizard Genomic DNA Purification Kit (Promega). Whole-genome library was constructed by Nextera DNA Library Preparation Kit (Illumina) and sequenced using an Illumina NextSeq 500 sequencing system. Thirty million single end reads were obtained. Reads were then aligned to *E. coli* K-12 MG1655 wild-type strain reference genome (NC_000913.2) using Bowtie2 and visualized using Integrative Genomics Viewer (IGV).

Plasmid construction

To construct the multi-sRNAs overexpression plasmid (pOE) the following sequence was used:
GAATTCCCTAGGCTGTGTCAACTCGTTATCAGTGCAGGAAAATGCCTGTTAGCGTAAAAGCAAAACAC
AAATCTATCCATGCAAGCATTCACCGCCGGTTTACTGGCGGTTTTTCGCCGTCATAAAAATCCTAGGGC
GGCCGCTCATAAAAAATTTATTTGCTTTGTGAGCGGATAACAATTATAATAATTGCTCACAACGGAGCG
GCACCTCTTTTAACCCTTGAAGTCACTGCCCGTTTCGAGAGTTTCTCAACTCGAATAACTAAAGCCAAC
GTGAACTTTTGCGGATCTCCAGGATCCTTTTTTTGCCATAAAAAAGCCCGCGGCCGCATCGATTCATAA
AAAATTTATTTGCTTTGTGAGCGGATAACAATTATAATAAAGTGGTGATAGAGGTATTGATAGGTGAAG
TCAACTTCGGGTTGAGCACATGAATTACACCAGCCTGCGCAGATGCGCAGGTTTTTGCCGGTCATCAA
TCTATCGATTGTACATCATAAAAAATTTATTTGCTTTGTGAGCGGATAACAATTATAATACAATCAAGATA
GAGGTATTGATTGGTGAGATTATTCGGTACGCTCTTCGTACCCTGTCTCTTGCACCAACCTGCGCGGAT
GCGCAGGTTTTTCGCACCTAATTTACTTGTACAACTAGTTCATAAAAAATTTATTTGCTTTGTGAGCGGA
TAACAATTATAATAATATCGTTAATCCGTCGTTGACTCCATGCCGATTCGGGTTAATCTGGTAGCGATC
CCCGTCGATACTTTTGACGAAGGCGGCAGGGATCGCAGAACTAGTAAGCTT.

The *in vitro* synthesized sequence (Hylabs) was cleaved by EcoRI and HindIII and ligated to the pQE80L plasmid cleaved by the same enzymes to yield plasmid pQE80L-sRNAsOE. The sRNAs expression levels were then validated by RT-qPCR.

Fitness calculations

The fitness index was calculated as described previously (Mitchell et al., 2009). Briefly, optical density was measured during growth and plotted versus time. Generation time was calculated for each biological replicate. The fitness index was then calculated by dividing the mutant generation time in exponential phase by the WT generation time.

Motility assay

Bacterial motility was examined by comparing the swimming ability of different strains on low-percentage agar plate. Briefly, biological triplicates from each strain were grown overnight at 30°C and 5 μl culture was inserted to the middle of a warm 0.25% soft agar plate that was incubated for 8 hours at 30°C. The swimming radius was measured (in pixels) using NIS-elements (Nikon). The ratio for each mutant compared to WT was calculated and plotted.

RT-qPCR

Total RNA was isolated and RNA concentrations were determined using a NanoDrop machine (NanoDrop Technologies). DNA was degraded by DNase treatment and equal concentration of 1 μg of DNA-free RNA were measured by Qubit fluorimeter (Invitrogen). The DNA-free RNA was then used for cDNA synthesis. cDNA was quantified by real-time PCR using SYBR-green mix in CFX Connect Real-Time system (Bio-Rad)

in 96-well plate module according to manufacturer instructions. Specific primers were designed for each target gene and the expression of each gene was normalized using *ssrA* levels. The relative amount of cDNA was calculated by comparative Ct method, and ΔCt was measured in triplicate. CFX maestro analysis software was used for conducting the analysis. For validation of the multi-sRNAs overexpression plasmid, the plasmid was transformed into the Δ5-1 strain and expression was induced with 0.1 mM IPTG.

Clinical strain isolation

The *E. coli* strain used for antibiotic treatments, RB001, was isolated from a clinical urine culture at Brigham and Women's Hospital (Boston, MA) in 2012. It was collected in a de-identified manner and approved by the Partners Health Care Institutional Review Board under Protocol #2012P001062

MIC determination

MICs were measured by standard broth microdilution assays (Wiegand et al., 2008) in Mueller Hinton broth (Difco).

Generation of RNA-Seq data

Illumina cDNA libraries were generated using RNAtag-Seq-TS (Bhattacharyya et al., 2019; Shishkin et al., 2015). Briefly, 250-500ng of total RNA was fragmented, depleted of genomic DNA, dephosphorylated, and ligated to DNA adapters carrying 5′-AN8-3′ barcodes of known sequence with a 5′ phosphate and a 3′ blocking group. Barcoded RNAs were pooled and depleted of rRNA using the RiboZero rRNA depletion kit (Illumina). Pools of barcoded RNAs were converted to Illumina cDNA libraries in 2 main steps: (i) reverse transcription of the RNA using a primer designed to the constant region of the barcoded adaptor with addition of an adapter to the 3′ end of the cDNA by template switching using SMARTScribe (Clontech); (ii) PCR amplification using primers whose 5′ ends target the constant regions of the 3′ or 5′ adaptors and whose 3′ ends contain the full Illumina P5 or P7 sequences. cDNA libraries were sequenced on the Illumina NextSeq 2500 platform to generate paired end reads.

Primary analysis of RNA-Seq data

Sequencing reads from each sample in a pool were demultiplexed based on their associated barcode sequence using custom scripts. Up to 1 mismatch in the barcode was allowed provided it did not make assignment of the read to a different barcode possible. Barcode sequences were removed from the first read as were terminal G's from the second read that may have been added by SMARTScribe during template switching. Reads were aligned to reference sequences using BWA (Li and Durbin, 2009) and read counts were assigned to genes and other genomic features using custom scripts. A single reference genome was used for analysis of each set of strains from the same species exposed to each drug. This reference genome was selected by aligning a subset of RNA-Seq reads for each strain in the bug-drug combination to all RefSeq genomes of that species and identifying the genome to which the highest percentage of reads aligned on average across all strains. Visualization of raw sequencing data and coverage plots in the context of genome sequences and gene annotations was conducted using GenomeView (Abeel et al., 2012).

QUANTIFICATION AND STATISTICAL ANALYSIS

All the experiments conducted for this study were performed in at least three biological replicates, and the data from each experiment were expressed as mean ± SEM (Standard Error of the Mean). Analysis of variance was performed using non-parametric Mann-Whitney test. p values <0.05 were considered significant. All statistical analyses were performed using the GraphPad Prism software version 6 (GraphPad Software, San Diego, California).